Roux's Arch Dev Biol (1996) 205:371–381

ORIGINAL ARTICLE

Hideki Katow · Shinji Komazaki

Spatio-temporal expression of pamlin during early embryogenesis in sea urchin and importance of *N*-linked glycosylation for the glycoprotein function

Received: 13 September 1995 / Accepted in revised form: 22 January 1996

Abstract Expression of pamlin, a heterotrimeric primary mesenchyme cell (PMC) adhesion glycoprotein, and its role during early embryogenesis were examined using immunochemistry and microinjection of pamlin to tunicamycin-treated embryos of the sea urchin, *Hemicentrotus pulcherrimus*. Pamlin faintly detected in egg cortex before fertilization was strongly expressed in the hyaline layer after fertilization. The embryonic apical surface retained pamlin throughout early embryogenesis, whereas pamlin on the basal surface showed a dynamic change of spatio-temporal distribution from morula to gastrula stage. Pamlin distributed on the entire basal surface of the ectoderm before onset of invagination gradually disappeared from the presumptive archenteron during gastrulation, and then was restricted to the apical tuft region and the PMC sessile sites in early gastrulae. Tunicamycin, an inhibitor of *N*-glycosydically linked carbohydrate formation, inhibited PMC migration and gastrulation. Tunicamycin also inhibited the assembly of mannose moieties of 180 and 52 kDa subunits of pamlin. Pamlin microinjection to the tunicamycin-treated embryos rescued them from this morphogenetic disturbance. PMCs did not bind to pamlin isolated from the tunicamycin-treated embryos. The present study indicated that pamlin plays an essential role in PMC migration, its termination and gastrulation, and the presence of *N*-glycosydically linked carbohydrate moieties that contain mannose are necessary to preserve the biological function of pamlin.

H. Katow (✉)[1]
Biology Laboratory, College of Science, Rikkyo University, Tokyo 171, Japan

S. Komazaki
Department of Anatomy, Saitama Medical School, Saitama 350-04, Japan

Present address:
[1] Asamushi Marine Biological Station, University of Tohoku, Aomori, Aomori 039-34, Japan

Key words Pamlin · Embryogenesis · Sea urchin · *N*-linked glycosylation · Glycoprotein

Introduction

In embryogenesis and specifically during the migration of embryonic cells, such as neural crest cells (e.g. Bronner-Fraser 1986; Hynes 1990; Humphries et al. 1991) and primordial germ cells (e.g. Hynes 1990), to the particular sites where they will undergo further differentiation the extracellular matrix (ECM) molecules that form the micro-environment play an essential role by providing an appropriate migratory substrate and some directional information (Newgreen 1990; Hynes and Lander 1992).

In sea urchin embryos, primary mesenchyme cells (PMCs) use ECM as their migration substrate (e.g. Karp and Solursh 1985; Katow 1986, 1987, 1990, 1995; Solursh 1986; Solursh and Lane 1988; Lane and Solursh 1988, 1991; Katow et al. 1990, 1991; Yamamoto et al. 1995), the protein pamlin in the basal lamina being a particularly good substrate (Katow 1995). PMCs migrate best on 2.5 μg/ml pamlin in vitro both lower and higher amounts of pamlin inhibit migration, suggesting that quantitative change of the protein plays a major role in PMC migration behaviour (Katow 1995).

PMCs actively migrate in mesenchyme blastulae and terminate their migration at two ventro-lateral sessile sites during the early gastrula stage (e.g. Katow and Nakajima 1992). The sessile site ectoderm has some morphologically distinct features, such as its triangular shape (Okazaki et al. 1962), ribosomal endoplasmic reticulum (rER) inflated with amorphous materials, frequent observation of exocytotic vesicles and mitochondrial accumulation on the basal side (Nakajima and Katow 1991). During migration, PMCs apparently associate with the fibrous component that is coated with amorphous ECM material in the basal lamina (Katow and Solursh 1979), or attach to the "Ca^{2+}-independent fibrils" (Amemiya 1989). Directional migration of PMCs

to the sessile sites in early gastrulae is not perturbed by the removal of the blastocoelic fluid (Katow 1990), suggesting that PMCs migrate using ECM that is fixed in the solid structure of the basal surface of the ectoderm, such as in the basal lamina. The basal lamina contains several large molecules, for example collagen (Wessel and McClay 1987), laminin (McCarthy et al. 1987) and pamlin (Katow 1995). If a basal lamina component has a guiding role to and ceases migration at particular embryonic sites without changing its molecular properties of PMC behaviour, one would expect the occurrence of the spatio-temporal distribution change to correlate with PMC behaviour alteration, such as the apparently random migration of PMCs in early mesenchyme blastulae to the prominent directional migration to the sessile sites in early gastrulae. Collagen and laminin do not change their locations with the alteration in PMC migration. To date, the only known basal lamina component that shows spatio-temporal alteration of distribution associated with the change of PMC migration behaviour is one that contains mannose moieties (Katow and Solursh 1982). Although several ECM components in the blastocoel have mannose moieties, it is pamlin which is the PMC adhesion protein. The PMC-binding activity of the protein is carried out by the 52 kDa subunit that contains the mannose moieties (Katow 1995).

In this study, the immunochemical expression and role of pamlin during early embryogenesis have been examined. The protein was present at the egg cortex in unfertilized eggs and was secreted to the hyaline layer after fertilization. This localization persisted through the gastrula stage.

The heterotrimeric configuration of this protein (Katow 1995) seen in unfertilized eggs was also preserved through the gastrula stage. Pamlin was seen in the cytoplasm associated with 0.5- to 0.8-μm-diameter granules before extracellular expression on the basal surface of the ectoderm from the swimming blastula stage. During the early gastrula stage, pamlin disappeared from the embryonic equator region and from the vegetal pole ectoderm region that will eventually form the archenteron. However, at PMC sessile sites and at the apical tuft region (that will provide archenteron attachment sites later on) the relative content of the protein increased.

Tanicamycin, an *N*-linked glycosylation inhibitor, inhibited PMC migration and attachment of the archenteron tip to the apical tuft basal surface. This antibiotic also perturbed the formation of the 180 kDa subunit and inhibited the mannosidation of the 180 and 52 kDa subunits of pamlin, causing a loss of the PMC-binding activity of the protein.

Materials and methods

Gametes of the sea urchin, *Hemicentrotus pulcherrimus*, were released by intracoelomic injection of 0.1 M acetylcholine chloride. The eggs were inseminated and raised in artificial sea water (ASW), Jamarin U (Jamarin Laboratory, Osaka), at 15° C.

Immunofluorescence microscopy

Eggs before insemination (unfertilized eggs), eggs 30 min after fertilization (fertilized eggs), morulae, swimming and mesenchyme blastulae, early and gastrulation half completed gastrulae (archenteron is half of the way to the animal pole) and 20 ng/ml tunicamycin-treated mesenchyme blastulae and early gastrulae were fixed in −20° C ethanol for 30 min and then embedded in Polywax (Polyscience, Warrington, Pa.) after one infiltration through an ethanol/Polywax mixture and two through pure Polywax at 40° C. Specimens were sectioned at 10 μm, dewaxed in pure ethanol, air-dried and rehydrated in 0.1 M phosphate-buffered saline (PBS). Sections were pre-incubated for 30 min with 3% bovine serum albumin (BSA) in 0.1 M PBS, rinsed with 0.1 M PBS, then incubated in a moist chamber for 4 h with the undiluted anti-pamlin monoclonal antibody, VIIIE6_2, that recognizes the 52 kDa subunit of the protein (Katow 1995). The specimens were then incubated for 1 h with rhodamine-labelled goat anti-mouse IgG serum (Jackson Immuno Research Lab., West Grove, Pa. 1:200 dilution in PBS). As a negative control, aliquots of sections were incubated with the culture medium of the hybridoma that did not produce VIIIE6_2 (instead of the mAb-containing culture medium), and were processed as stated above. Micrographs were taken using Kodak Tri-X film.

Image analysis of pamlin localization

Immunohistochemical micrographs of unfertilized eggs, eggs 30 min after fertilization, mesenchyme blastulae and gastrulation half completed gastrulae prepared as stated above were image-analysed using an EPA-3000 Densito-Pattern Analyzer (Maruzen Petrochemical Co. Ltd., Tokyo). The traces of the sensor scanning for mesenchyme blastulae and gastrulation half-completed gastrulae are shown in Fig. 2.

Immunoaffinity purification of pamlin

One volume of unfertilized and fertilized eggs (30 min after fertilization) was lysed in 6 vol of the lysis buffer (6 M urea, 1% Nonidet P-40, 10 mM TRIS-HCl, pH 7.6; Shimizu-Nishikawa et al. 1990), respectively, and were mixed with 3 vol of −20° C pure ethanol. The samples were left for a few days at −20° C. The ethanol precipitates were washed a few times with −20° C ethanol, and air-dried at 4° C. These powdered samples were stored at −50° C until use.

ECM from swimming and mesenchyme blastulae, early gastrulae, and 20 ng/ml tunicamycin-treated mesenchyme blastulae were collected as described before (Katow 1995), and stored at −50° C until use.

Pamlin was affinity purified using an Immunopure (G) IgG purification kit (Piers, Rockford, Il). VIIIE6_2 was concentrated by ×35 with a Centricon 10 concentrator (Amicon Inc., Beverly, Mass.), and was bound to a 3 ml protein G-coated beaded agarose column with 0.1 M sodium acetate buffer (pH 5.0), and 5 mg/ml of fertilized and unfertilized egg lysate, blastocoelic ECM samples from swimming and mesenchyme blastulae, early gastrulae, and tunicamycin-treated mesenchyme blastulae were loaded, respectively. Pamlin was eluted with 0.1 M glycine-HCl buffer (pH 2.7) according to the manufacturer's instructions, and was concentrated by ×30.

These immunoaffinity purified pamlins were separated with 10% sodium dodecyl sulphate-polyacrylamide gel electrophoresis (SDS-PAGE) slab gels under reduced condition. The gels were stained with a Bio Rad silver stain kit according to the manufacturer's instructions. Aliquots of gels were stained with Coomassie brilliant blue (CBB). Apparent M_r values were estimated by comparison with prestained molecular weight standards (GIBCO BRL) whose apparent M_r values were calculated batch by batch by the manufacturer.

Tunicamycin treatment and microinjection of pamlin

The eggs were fertilized in normal ASW, immediately transferred to 20 ng/ml tunicamycin dissolved in ASW (tunicamycin-ASW), and incubated until the aliquots of embryos that were incubated in normal ASW reached gastrula stage. The tunicamycin-treated embryos were examined under a Nikon inverted phase-contrast microscope without fixation.

The immunoaffinity-purified pamlin from normal mesenchyme blastulae was dissolved in tunicamycin-ASW at 28 μg/ml and 112 μg/ml, respectively. About 0.3 nl of each pamlin solution was microinjected to 13 swimming blastulae for 28 μg/ml pamlin and 10 swimming blastulae for 112 μg/ml pamlin. The embryos were incubated in tunicamycin-ASW in a 200 μl small chamber until the control embryos (that were incubated in normal ASW) reached gastrula stage at 15° C. Each chamber contained one embryo. The embryos were examined under an inverted phase-contrast microscope without fixation.

PMC binding assay on pamlins in vitro

PMCs were isolated from mesenchyme blastulae according to the method described previously (Katow and Hayashi 1985). Pamlins from normal mesenchyme blastulae and the tunicamycin-treated mesenchyme blastulae (T-pamlin) were dissolved in double distilled water at 2.5 μg/ml, pipetted into 24-well plastic plates, and were made to coat the bottom of the plastic wells by incubating overnight at 4° C. PMCs (3×10^4) were suspended in normal ASW and applied to 5-mm-long and 2.4-mm-inner diameter microglass tubes stood in the middle of each ASW-filled well. PMCs were allowed to settle for 30 min and then the tubes were gently pulled up to minimize turbulence of the medium that could potentially dislocate the PMCs. PMCs were then incubated for 2 h at 20° C and fixed with OmniFix (Polyscience), stained with 0.01% amido black 10B for 5 min, washed briefly with amido black 10B destained solution, and air-dried for 30 min. The PMCs on the plastic plates were examined under a dissection microscope.

Immunoblotting analysis

The ECMs from normal mesenchyme blastulae and from tunicamycin-treated mesenchyme blastulae were prepared as stated earlier. The samples were loaded and separated on 10% SDS-PAGE gels under reducing condition (Laemmli 1970), and were electrophoretically transferred to nitrocellulose filters according to Towbin et al. (1979). The nitrocellulose blots were incubated with TBS [0.05 M TRIS-HCl (pH 7), 0.15 M NaCl and 0.05% Tween-20] containing 5% BSA for 1 h. The nitrocellulose blots were incubated with $VIIIE6_2$ in undiluted hybridoma culture medium for 1 h, and then with alkaline phosphatase-conjugated goat anti-mouse IgG (Promega Biotech., Madison, Wis.) (1:7500 dilution) for 1 h. The immunoreaction was visualized according to the manufacturer's instructions.

Concanavalin A binding assay

To examine tunicamycin effects on mannose moieties in pamlin, normal and T-pamlins were loaded and separated on 10% SDS-PAGE gels under reducing conditions. The concanavalin A (Con A) binding assay was carried out by the method described before (Katow 1995). Briefly, the gels were fixed in a mixture of 25% isopropanol and 10% acetic acid overnight on a rocker, rinsed in 0.1 M PBS overnight, and then incubated with 0.5 mg/ml Con A from *Canavalia ensiformis*, type V (Sigma) for 2 h. The gels were then rinsed in 0.1 M PBS overnight with several changes during the period and incubated for 2 h with 50 μg/ml horseradish peroxidase (Wako Pure Chemicals). The gels were rinsed in 0.1 M PBS overnight with several changes during the period, and the Con A binding sites were visualized with 0.5 mg/ml diaminobenzidine DAB; Sigma).

Results

Expression of pamlin from unfertilized eggs to early gastrulae

In unfertilized eggs, pamlin was localized at the egg cortex region associated with granules of about 0.5 μm diameter (Fig. 1A, inset), and the intensity of the pamlin signal was not strong (Fig. 1A, B). Thirty minutes after fertilization, all the pamlin signal shifted to the hyaline layer and had a considerably high intensity (Fig. 1C, D). According to the image analysis using a Densito-Pattern Analyzer, the intensity of the pamlin signal in the hyaline layer was about 3–4 times higher than that in the unfertilized eggs (data not shown). No cytoplasmic signal was seen after fertilization, suggesting that pamlin was secreted during fertilization to the hyaline layer. The hyaline layer pamlin was seen throughout the gastrula stage. Previous immunoblotting results suggest that pamlin signals seen on both the basal and apical surfaces of embryonic ectoderm are from the same molecule (Katow 1995).

The restoration of the cytoplasmic pamlin signal was seen in morulae, in which pamlin was sporadically visible at the apical and basal sides (Fig. 1E inset, F). These pamlin signals were associated with 0.5- to 0.8-μm-diameter granules.

In swimming blastulae, the basal surface of the ectoderm showed a distinctive pamlin signal, although morphologically its distribution was sporadic (Fig. 1G, H). Cytoplasmic pamlin increased, associated with the 0.5- to 0.8-μm-diameter granules (Fig. 1G, inset).

In mesenchyme blastulae, pamlin was prominently and evenly seen on the entire basal surface of the ectoderm as has been described before (Katow 1995) (Fig. 2A, B). According to the Densito-Pattern analysis, the intensity of pamlin signal on the basal surface was indistinguishable from place to place (Fig. 2M). The samples incubated as a negative control did not show any second antibody binding (Fig. 2C, D).

In gastrulation half completed gastrulae, the basal surface of the ectoderm showed several pamlin-free regions (Fig. 2K, L). Pamlin was mainly restricted to two regions, a region around the base of the invaginating archenteron (RABarch), and a region of the animal pole ectoderm (RAPecto; Fig. 3). At RABarch, the pamlin-positive area widened beneath the PMC aggregate, whereas on the other side of the archenteron that locates the PMC cable, the pamlin-positive area was narrowed (Fig. 2K). A minor pamlin-positive region was present at the tip of invaginating archenteron. This region formed a distinctive patch with a strong pamlin signal. Several archenteron tip cells around the pamlin-positive patch extended cell processes to RAPecto. A few secondary mesenchyme cells attached to the RAPecto. The Densito-Pattern analysis showed that the intensity of the pamlin signal at RABarch was slightly (about 40%) stronger than that at RAPecto, and RAPecto showed an about 20%

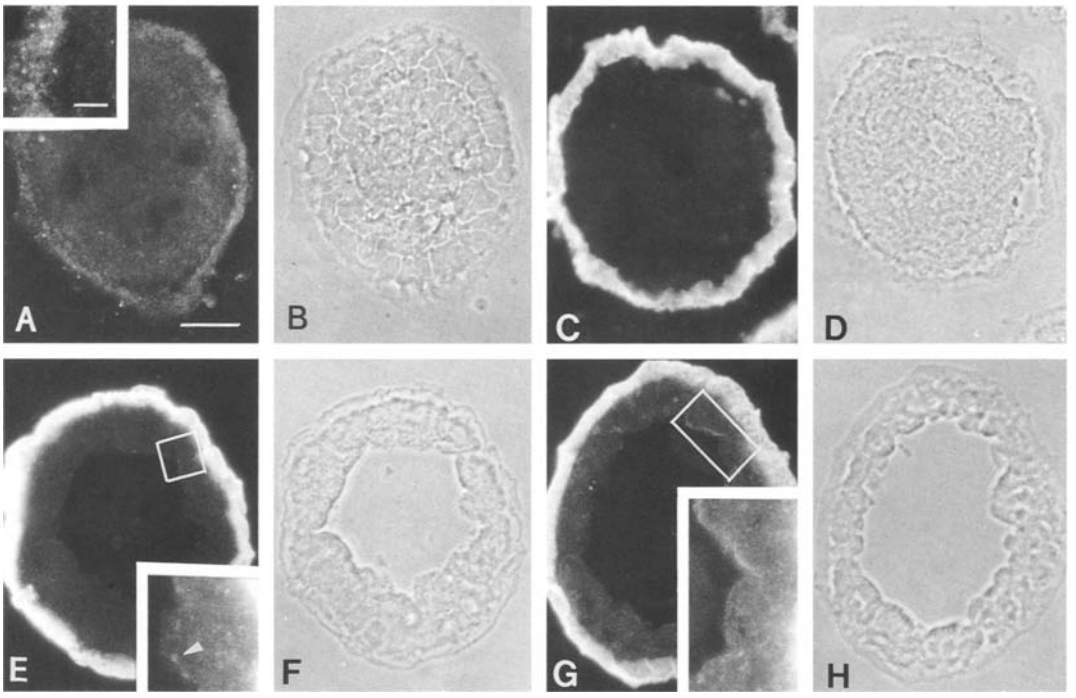

Fig. 1A–H Immunohistochemistry of pamlin. Pamlin is weakly detected in unfertilized eggs at the cortex region, associated with granules of about 0.5 μm diameter (**A**, *inset*). Thirty minutes after insemination, pamlin is strongly detected in the hyaline layer (**C**). In morulae, pamlin is localized in the hyaline layer, but not on the basal surface of the ectoderm (**E**). In cytoplasm on the basal side, pamlin is associated with 0.7–0.8 μm diameter granules (**E** *inset, arrowhead*). Swimming blastulae are the youngest stage in which pamlin is first detected on the basal surface of the ectoderm; the protein is sporadically detected on the basal surface of the ectoderm (**G**) and in the cytoplasm (**G** *inset*). **B**, **D**, **F** and **H** are phase-contrast micrographs of **A**, **C**, **E** and **G**, respectively. A *square* in **E** and a *rectangle* in **G** show the location of each inset, respectively. *Bars* in **A** and **A** *inset* show 20 and 3 μm, respectively

stronger fluorescence than the archenteron patch (Fig. 2K, O, P). In contrast to these regions, pamlin was not seen in a large equator region of ectoderm (ERecto; Fig. 2K, N). The Densito-Pattern analysis also showed that pamlin signals at RABarch and RAPecto were about four times stronger than those seen on the entire basal surface in mesenchyme blastulae (Fig. 2M, O), suggesting that the occurrence of these pamlin-positive areas is associated with not only the local decline of the protein at ERecto and the archenteron surface but also with the local increase of pamlin at RAPecto and RABarch. Thus, the basal surface of early gastrulae was divided into five different regions, creating a heterogeneous basal lamina in terms of pamlin presence (Fig. 3).

The occurrence of this heterogeneity in the basal lamina took a process of gradual rearrangement during the early gastrulation period. According to a series of histochemical investigations conducted during the period from late mesenchyme blastula stage to early gastrula stage, with shorter intervals than the above study, the sporadic disappearance of the pamlin signal was seen in the vegetal pole ectoderm when it showed a slight sign of indentation prior to invagination (Fig. 2E, F). At this moment, pamlin was still well retained in a large area of the embryonic equator. However, in the vegetal pole ectoderm a large number of pamlin-positive signal granules appeared, and the signal beneath the PMC sessile sites intensified.

Fig. 2 Immunohistochemistry of pamlin from mesenchyme blastula stage to gastrulation half completed gastrula stage (**A–L**) and comparative analysis of pamlin distribution by a Densito-Pattern Analyzer (**M–P**). Anti-pamlin monoclonal antibody (mAb) bound to the entire basal lamina of mesenchyme blastulae (**A**, **B**), whereas the control medium (hybridoma culture medium whose hybridoma does not produce anti-pamlin mAb) did not bind to any feature of mesenchyme blastulae (**C**, **D**), showing the specificity of anti-pamlin mAb binding to the basal lamina and hyaline layer. Even distribution of pamlin in the basal lamina in mesenchyme blastulae is disrupted at the vegetal pole ectoderm region when the region shows a slight indentation before the occurrence of invagination (**E**, **F**). Cytoplasm of this region contains anti-pamlin mAb-positive granules. The further the invagination proceeds, the less basal surface pamlin is detected (**G**, **H**). In contrast, the intensity of the pamlin signal increases at the periphery of the invaginating archenteron (**G**). In early gastrulae, pamlin is restricted to the area around the invaginating archenteron, that includes the primary mesenchyme cell (PMC) sessile sites (**I**, **J**), but a new pamlin-positive spot appears at the tip of the invaginating archenteron (**I**). In gastrulation half-completed gastrulae, pamlin is mainly restricted to two areas: the area around the invaginating archenteron and the apical tuft region (**K**, **L**). Pamlin apparently spreads wider beneath the PMC aggregate (**K**, *pamlin-positive area on the left*) than at the PMC cable (**K**, *pamlin-positive area on the right*). The protein is not detected in any other areas, except for a spot at the tip of invaginating archenteron (**K**, **L**). **B**, **D**, **F**, **H**, **J** and **L** are phase-contrast micrographs of **A**, **C**, **E**, **G**, **I** and **K**, respectively (*bar* 20 μm). *White lines with letters M, N, O* and *P* (**A**, **K**) show where the censor of a Densito-Pattern Analyzer has scanned. Numbers printed by each white line correspond to those in **M–P**. **M–P** Results of scans shown as *white lines M–P* in **A** and **K**

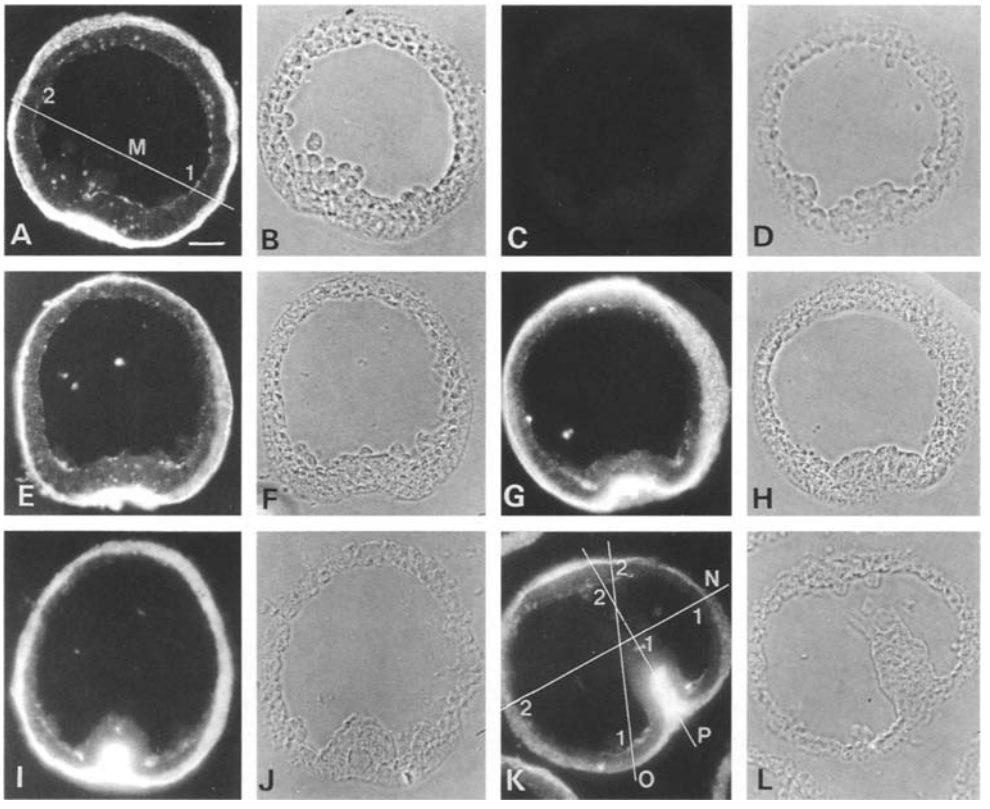
A
B
C
D
E
F
G
H
I
J
K
L
M
N
O
P
1
2

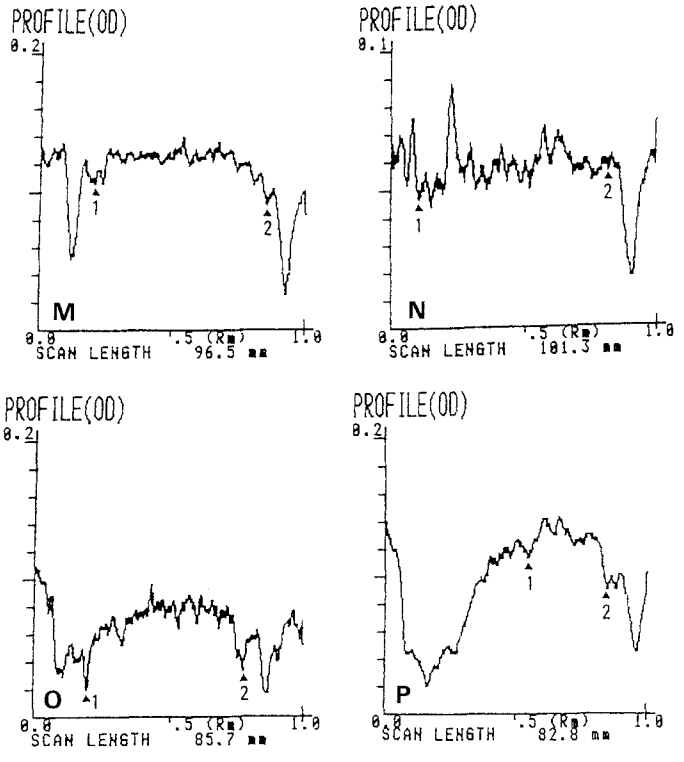
PROFILE(OD)
M
N
O
P
SCAN LENGTH
96.5
101.3
85.7
82.8

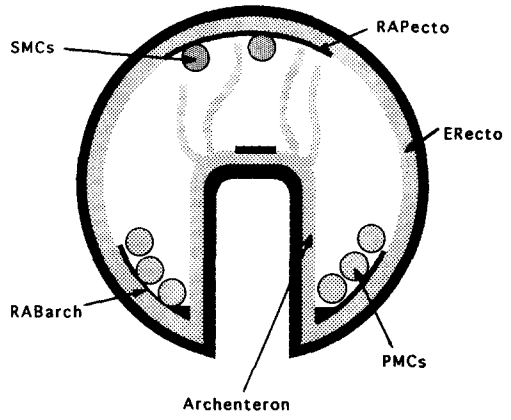

Fig. 3 A schematic indication of pamlin distribution in an early gastrula. After rather even distribution of pamlin in younger embryos, the protein distribution is restricted to three regions, a region around the base of the archenteron (*RABarch*), a region of animal pole ectoderm (*RAPecto*) and a tiny spot on the leading edge of the invaginating archenteron. Pamlin disappears from most of the embryonic equatorial region (*ERecto*; *PMCs* primary mesenchyme cells, *SMCs* secondary mesenchyme cells)

In embryos that showed further invagination, the pamlin signal was scarcely seen on the surface of vegetal pole ectoderm (Fig. 2G, H) and in a large area of animal hemisphere. In contrast, the signal further intensified at PMC sessile sites (RABarch).

In gastrulation one-third-completed gastrulae (early gastrulae), pamlin was seen only at the PMC sessile sites (Fig. 2I, J), and at a very small spot at the tip of archenteron that appeared during gastrulation. These observations indicate that pamlin disappearance at the vegetal pole region is associated with the progress of invagination.

At RABarch, tangential histological sections showed the presence of two pamlin-positive patches associated with the PMC aggregating area (Fig. 4A, B). These pamlin-positive areas had PMCs located on them (Fig. 4A, asterisks). This observation was consistent with the side view section in Fig. 2K, and showed that the pamlin-positive area did not extend through the entire RABarch, but was wider at the two PMC sessile sites and narrowed in between (see schematic diagram, Fig. 4C).

Thus, pamlin distribution on the basal surface altered quite dynamically during early embryogenesis. This vicissitude of pamlin expression was categorized into three groups: (1) from signal-positive to negative at ERecto and the basal surface of the archenteron, (2) intensification of the signal at RABarch, and (3) the rather short-lived reverse changes from signal-positive to negative and again to positive at RAPecto and at a small area of the archenteron tip.

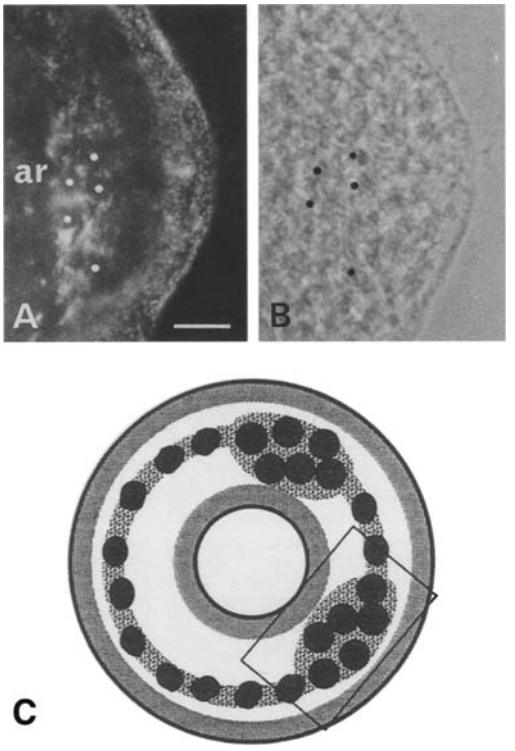

Fig. 4A–C Immunohistochemistry of a tengential section at a PMC sessile site in an early gastrula. **A** PMCs aggregate on a patch of pamlin that is formed by the archenteron (*ar*; *small asterisks* PMCs). **B** A phase-contrast micrograph of **A**. *Black asterisks* show PMCs corresponding to those in **A**. **C** Schematic diagram; *rectangle* shows the histological location of **A** (*black dots* PMCs, *shadowed pattern* pamlin-positive areas, *central smaller circle* archenteron, *bar* 20 μm)

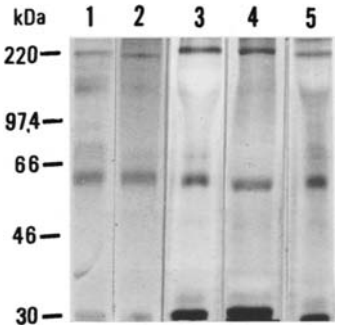

Fig. 5 Silver-stained 10% SDS-PAGE gel analysis of pamlins immunoaffinity-purified from whole cell lysate of unfertilized eggs (*lane 1*) and eggs 30 min after fertilization (*lane 2*), extracellular matrices from swimming (*lane 3*) and mesenchyme blastulae (*lane 4*), and early gastrulae (*lane 5*). The heterotrimeric molecular configuration is apparently identical among these pamlins. The *numbers on the left side* show relative molecular weight standards (kDa)

Molecular configuration during development

The heterotrimeric configuration of pamlin was preserved throughout the early gastrula stage (Fig. 5). In unfertilized eggs, although a faint braod band was seen between the 180 and 52 kDa bands (Fig. 5, lane 1), a 3-band feature was clearly seen, suggesting that the subunit configuration of pamlin is already established in unfertilized eggs. In fertilized eggs, pamlin showed a quite

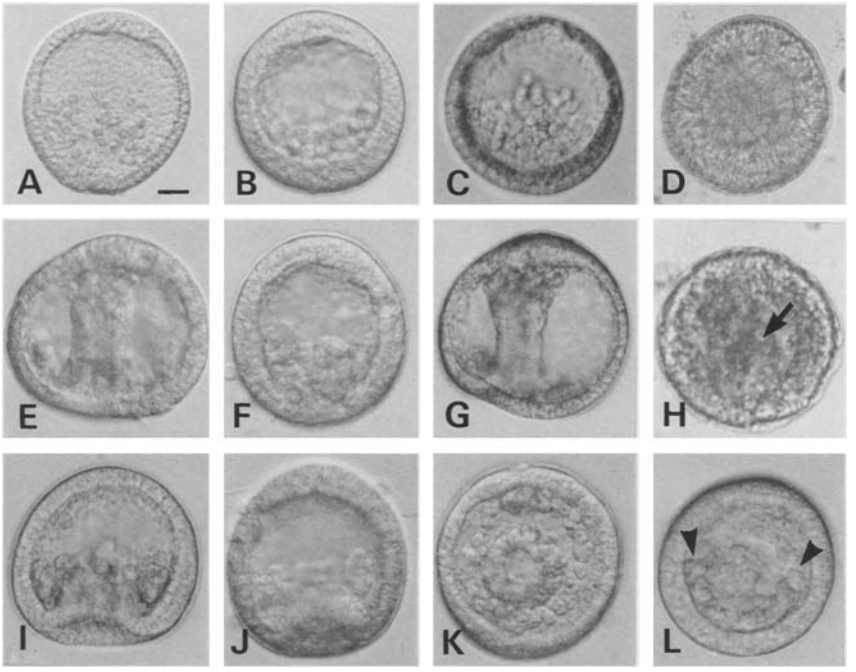

Fig. 6A–L Rescue of morphogenesis in tunicamycin-treated embryos by microinjection of pamlin. **A** and **E** are a normal mesenchyme blastula and gastrula, respectively, incubated in normal artificial sea water (ASW). PMC migration (**A**) and complete gastrulation (**E**) did not occur in embryos incubated with 20 ng/ml of tunicamycin (**B** and **F**, respectively). An adequate amount of pamlin (0.3 nl of 28 μg/ml) injected to the blastocoel of swimming blastulae rescued them from this morphogenetic disturbance: **C** PMC migration rescue, and **G** gastrulation rescue. Injection with too high an amount of pamlin (0.3 nl of 112 μg/ml) caused no PMC migration (**D**) and incomplete gastrulation (**H**), respectively; the PMCs formed a clump in these embryos and invagination of the archenteron was limited (**H**, *arrow*). **J** Tunicamycin did not inhibit the initial invagination, but strongly inhibited further progress. **L** Polar view of the tunicamycin-treated embryo showing the disturbed PMC cable formation (*arrowheads*). **I** and **K** show a side view and polar view of normally developed early gastrulae, respectively (*bar* 20 μm)

similar molecular configuration to that seen in embryos (Fig. 5, lane 2). However, the non-specified minor high-molecular-weight band seen between the 180 and 52 kDa subunits in unfertilized eggs was still faintly seen. The band was also faintly seen in embryonic pamlins, but was not stained with CBB (data not shown). In swimming (Fig. 5, lane 3) and mesenchyme blastulae (Fig. 5, lane 4) and in early gastrulae (Fig. 5, lane 5), the heterotrimeric molecular configuration of pamlin was well preserved and was apparently consistent throughout the developmental period, suggesting that the alteration of pamlin distribution was not associated with a change of molecular configuration.

Tunicamycin-induced morphogenetic disturbance and restoration by pamlin injection

Pamlin has mannose-containing sugar moieties at its 52 and 180 kDa subunits, the 52 kDa subunit being the active PMC binding site of the protein (Katow 1995). To examine the role of the sugar moieties of pamlin, tunicamycin, an antibiotic and a potent inhibitor of *N*-glycosydically linked carbohydrate, that includes mannose (Struck and Lennarz 1981), was used.

Since tunicamycin is not metabolized in vivo or in vitro (Struck and Lennarz 1981), the antibiotic was externally applied to the fertilized eggs and they were incubated in tunicamycin-ASW until the control embryos incubated in tunicamycin-free ASW reached mesenchyme blastula (Fig. 6A) or gastrula stage (Fig. 6E). The embryos in tunicamycin-ASW formed PMCs but they piled up where they had ingressed and did not migrate in the mesenchyme blastula stage (Fig. 6B). In gastrulae, the initial invagination occurred in tunicamycin-treated embryos but the archenteron only elongated up to one third to one-half of the way to the animal pole (Fig. 6F).

This morphogenetic disturbance may simply be caused by a cytotoxic effect of tunicamycin (e.g. Struck and Lennarz 1981). Even if this is not the case, there could be many *N*-glycosylated glycoproteins in the blastocoel of the embryos that potentially play a more crucial role in morphogenesis than pamlin does. To sort out these possibilities, pamlin was microinjected to swimming blastulae under the influence of tunicamycin. In all 13 28 μg/ml-pamlin-injected embryos in tunicamycin-ASW, PMC migration (Fig. 6C) and gastrulation (Fig. 6G) were restored, indicating that the tunicamycin-caused morphogenetic disturbance was not due to a cytotoxic effect, and that pamlin could reverse the tunicamycin-induced morphogenetic disturbance. This also suggests that *N*-glycosydically linked sugar moieties play an essential role in the function of pamlin. In vitro pamlin has an optimum concentration to promote PMC migration (Katow 1995), suggesting that an inadequate amount of pamlin may cause some morphogenetic disturbance or

would not rescue the tunicamycin-induced inhibition of embryogenesis in vivo. In embryos that were injected with four times higher amounts of pamlin (112 μg/ml), PMCs did not migrate but formed a tightly clumped cell mass in the blastocoel (Fig. 6D), and gastrulation ceased at the initial stage of invagination (Fig. 6H, arrow). Two of the ten embryos formed a densely packed cell clump without gastrulation. All ten embryos, however, were swimming actively. These observations indicated that pamlin also has an optimum concentration for in vivo morphogenesis.

In early gastrulae in which the archenteron invaginated about half of the way to the animal pole (Fig. 6I) and PMCs aggregated at two ventro-lateral sites and surrounded the archenteron with a PMC cable formed in between (PMC ring; Fig. 6K), tunicamycin-treated embryos did not form the PMC aggregates (Fig. 6J, L) and PMC cable formation was incomplete due to a disrupted cell chain in places (Fig. 6L, arrowheads). This suggests that tunicamycin caused not only inhibition of PMC migration and incomplete gastrulation but also incomplete PMC patterning. These severe disturbances of morphogenesis by tunicamycin treatment may be due to the disappearance of pamlin from the basal lamina.

To examine this possibility, we have conducted immunohistochemical investigations of pamlin in tunicamycin-treated embryos. In these embryos, however, pamlin was detected on the basal lamina both in mesenchyme blastulae (Fig. 7A, B) and early gastrulae (Fig. 7C, D), indicating that the apparent histological distribution of pamlin was not visibly affected by the antibiotic. This also suggests that it could be the molecular properties of pamlin that are disturbed.

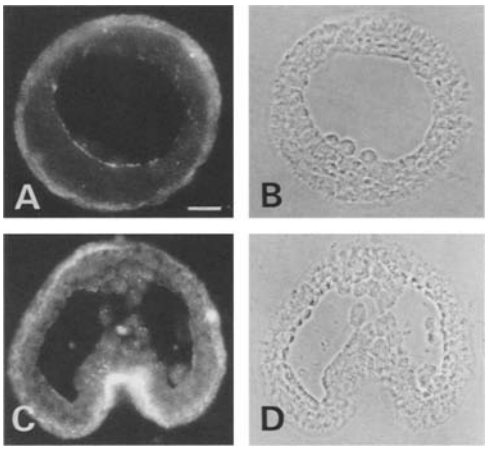

Fig. 7A–D Immunohistochemistry of a tunicamycin-treated mesenchyme blastula (**A**, **B**) and early gastrula (**C**, **D**). Pamlin was localized at normal histological positions despite the lack of PMC migration in the mesenchyme blastula (**A**, **B**) and PMC pattern formation in the early gastrula (**C**, **D**). **B** and **D** are phase-contrast micrograms of **A** and **C**, respectively (*bar* 20 μm)

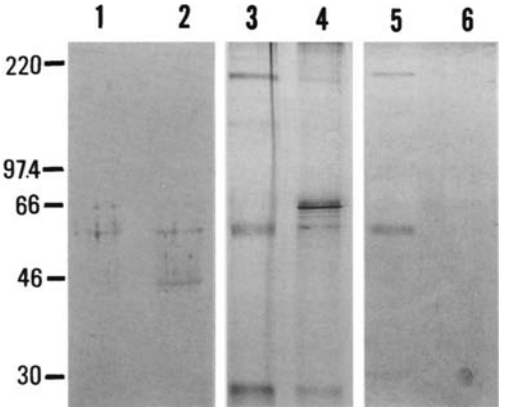

Fig. 8 Effects of tunicamycin on molecular properties of pamlin. Immunoblottings of normal pamlin (*lane 1*) and tunicamycin-treated pamlin (T-pamlin; *lane 2*), silver stains of immunoaffinity-purified normal pamlin (*lane 3*) and tunicamycin-treated pamlin (*lane 4*), and Con A binding assay to normal pamlin (*lane 5*) and tunicamycin-treated pamlin (*lane 6*). Tunicamycin treatment caused the production of a major 68-kDa fragment and two minor, smaller fragments instead of the 180 kDa subunit

Molecular properties of T-pamlin

The earlier immunohistochemistry indicated that the immunological epitope of VIIIE6$_2$ was preserved in T-pamlin, suggesting that it would be possible to isolate T-pamlin with the normal pamlin-affinity column. Thus, immunochemically detectable properties of the T-pamlin were examined by immunoblotting and immunoaffinity purification of the protein. On the immunoblot, unlike normal pamlin (Fig. 8, lane 1), the immunoreaction of T-pamlin (Fig. 8, lane 2) was associated with an additional VIIIE6$_2$-positive band at about the 47 kDa region, suggesting that tunicamycin treatment had caused the degradation of VIIIE6$_2$ epitope in the 52 kDa subunit of the protein.

Silver-stained 10% SDS-PAGE gel analysis indicated further degradation of pamlin at the 180 kDa subunit (Fig. 8, lanes 3 and 4). In this study, three new bands appeared around the 68 kDa region as one major band and two smaller minor bands that were very close to the major band, and the 180 kDa subunit disappeared (Fig. 8, lane 4) indicating that the 180 kDa subunit was not fully formed in T-pamlin. The 52 kDa subunit also considerably declined in amount, supporting the immunoblotting results. The 23-kDa subunit was not visibly changed. However, the 47-kDa fragment seen in immunoblotting was not detected in this analysis (Fig. 8, lane 4) nor in CBB-stained gel analysis (data not shown), suggesting that a part of the VIIIE6$_2$ epitope is shared by material that is not stained by silver or CBB. This indicated that tunicamycin only affected the mannose-containing subunits of pamlin (Katow 1995), and suggested that the mannose moieties of these subunits may be removed by tunicamycin treatment.

A Con A binding assay applied to 10% SDS-PAGE gel-separated pamlin confirmed the assumption. Both 180 and 52-kDa subunits lost the Con A binding property (Fig. 8, lanes 5, 6), indicating that mannose moieties had been lost from these subunits.

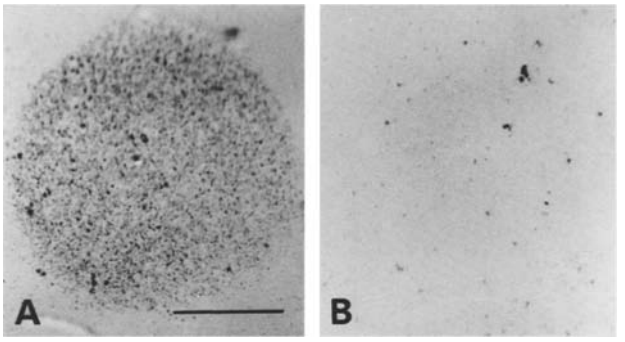

Fig. 9A, B PMC-adhesion assay on pamlin. PMCs attached to normal pamlin (**A**), but not to the T-pamlin substrate (**B**) (*bar* 1 cm)

PMC adhesion activity of T-pamlin

In vitro pamlin maximally promotes PMC migration at 2.5 μg/ml (Katow 1995). To examine the PMC adhesion activity of T-pamlin in vitro, PMCs were incubated on 2.5 μg/ml of normal pamlin or of T-pamlin. Consistent with the previous observation, PMCs on normal pamlin attached well to the substrate and actively migrated during the 2 h incubation period (Fig. 9A), whereas PMCs did not attach to T-pamlin and peeled from the substrate during fixation (Fig. 9B). So by removing the mannose moieties and severely disturbing the molecular configuration of the protein, tunicamycin effectively destroys the PMC-binding activity of pamlin.

Discussion

The present study showed that pamlin was immunologically detected in unfertilized eggs as an exocytotic component associated with granules of about 0.5 μm diameter at the egg cortex. The size of these granules was about half that cortical granules (Giudice 1973) and acidic vesicles (Lee and Epel 1983), and unlike cortical granules, these pamlin-positive granules did not lie in a single row. Although electron microscopy is needed to elucidate exactly how the pamlin signal shifts to the extracellular space, it is possible to see by light microscopy that, like fibropellins (Bisgrove and Raff 1991), pamlin is secreted after fertilization, though fibropellins are secreted solely to the hyaline layer and not to the basal lamina.

Pamlin was not detected in the blastocoel of morulae. Basal surface pamlin was seen after detection of the protein in ectodermal cytoplasm associated with 0.5- to 0.8-μm-diameter granules. These granules were seen throughout the mesenchyme blastula stage in which pamlin was fully expressed on the basal surface; it disappeared from the vegetal pole ectoderm during the early period of gastrulation. Previous immunoblotting results showed that pamlins seen on the apical and basal surfaces had the same molecular configuration (Katow 1995).

The present unchanged molecular configuration of immunoaffinity-purified pamlin from unfertilized eggs through to early gastrulae indicates that immunochemically detected pamlin signals are all caused by a similar molecule. Thus, it was suggested that, like some extracellular matrix molecules in echinoderm embryos (e.g. McClay 1993), at least a part of the pamlin molecule could be transported from the hyaline layer to the basal lamina through the cytoplasm in association with the vicissitudes of cell surface expression pattern. However, this does not exclude the possibility of local de novo synthesis of pamlin, as will be mentioned later.

After a process of relocation, pamlin was restricted to three regions: RABarch, RAPecto and a small area at the archenteron tip. PMCs are localized in RABarch, and more specifically in two areas of the pamlin substrate. According to Densito-Pattern analysis in this paper, the RABarch contains about four times the amount of pamlin than does the basal lamina in mesenchyme blastulae, suggesting local de novo synthesis of pamlin.

Although we do not know exactly how much pamlin is contained in the basal lamina of mesenchyme blastulae, it would seem obvious that this lamina provides a good PMC migration substrate, whereas the PMC sessile sites contain amounts of pamlin in excess of that needed for PMC migration. Based on the observations: (1) that PMCs retain motility at PMC sessile sites after the formation of PMC aggregates (Katow and Nakajima 1992); (2) that PMCs migrate best on 2.5 μg/ml pamlin; (3) that both half lower and about two times higher (than 2.5 μg/ml) amounts of pamlin inhibit PMC migration (Katow 1995); (4) that ERecto and the archenteron surface contain amounts of pamlin, undetectable by immunohistochemistry, that are too low and, on the contrary, RABarch and RAPecto contain amounts that are too high for PMC migration; and (5) that PMCs aggregate on the pamlin-rich patch in RABarch, it would appear that pamlin at the PMC sessile sites does not provide suitable substrate conditions for PMC migration.

Thus, these results strongly suggest that PMC migration terminates not due to the lowered motility of the cells but due to the occurrence of a poor migration substrate. PMC localization at the two ventro-lateral sessile sites occurs due to PMC retraction away from the basal surface, a poor migratory substrate, and their subsequent entrapment in the pamlin-rich substrate areas (which are also a poor migratory substrate in early gastrulae). The gradual disappearance of pamlin at ERecto would send PMCs to the pamlin-positive RABarch, and once PMCs gathered in this region, pamlin-rich conditions would acively prevent the PMCs from migrating away.

The mechanism of pamlin disappearance, particularly from the vegetal pole ectoderm during gastrulation, may be associated with the differentiation of the endoderm. It correlates with an expression of Endo 16, an endodermal cell-specific protein, on the invaginating archenteron surface during endoderm differentiation (Soltysik-Espanola et al. 1994), suggesting that pamlin is being replaced by Endo 16, but the present study does not allow any further implications about the mechanism to be made.

It is known that *N*-linked glycosylation inhibition, e.g. by tunicamycin, disturbs sea urchin embryogenesis (e.g.

Heifetz and Lennartz 1979; Welply et al. 1985), thus implicating the importance of *N*-linked glycoproteins in sea urchin embryogenesis. As in previous tunicamycin experiments (e.g. Hames 1990), the antibiotic effectively inhibited early embryogenesis in the *H. pulcherrimus* embryo. This morphogenetic disturbance brings in numerous *N*-linked glycoproteins as potential candidates for having an important role in morphogenesis. In this study, however, tunicamycin-induced morphogenetic disturbance was effectively reversed by a sole microinjection of pamlin, indicating that this *N*-linked glycoprotein is the one that plays a major role in early embryogenesis, and more particularly in PMC migration promotion, its termination at particular sites, and the attachment of the archenteron to the apical tuft region. The latter region is reported to be a target of filopodia extended by secondary mesenchyme cells that are embedded in the tip of the archenteron during gastrulation (Hardin 1988; Hardin and McClay 1990). Pamlin provides appropriate ECM substrate conditions for these morphogenetic events. this was also confirmed by the observation that the formation of the PMC cable was severely disturbed by tunicamycin treatment. A high dose microinjection of pamlin under the influence of tunicamycin did not reverse this abnormal morphogenesis but caused the formation of a tightly packed PMC clump without PMC migration and the failure of archenteron tip attachment to the apical tuft region. This suggests that the correct amount of pamlin needs to be provided for normal in vivo morphogenesis to take place.

Pamlin was initially expressed extracellularly on the fertilized egg surface, (which becomes the apical surface of later embryonic stages) then it shifted to the basal lamina being associated with the appearance of cytoplasmic granules of about 0.5 μm diameter during early embryogenesis. This apparently suggests that the expression of basal lamina pamlin is the consequence of intracytoplasmic transportation from the apical surface to the basal lamina. However, based upon the report that the rate of incorporation of [^{3}H]Man into oligosaccharylpyrophosphoryldolichol and into protein increases three to four times before gastrulation (Welply et al. 1985), the activity of glycosyl transferases that are responsible for *N*-linked glycosylation must increase considerably too. Thus, intracytoplasmic transportation may not be the only factor responsible for basal lamina expression of pamlin, and it is possible that de novo synthesis is involved to some extent. The latter appears a particularly likely explanation for the increased amount of pamlin (four times compared to the mesenchyme blastula stage) at PMC sessile sites in early gastrulae. The well-inflated rER seen on the basal side of the PMC sessile site ectoderm (Nakajima and Katow 1991) also suggests an intensification of formation of local ECM, including pamlin.

The tunicamycin treatment did not completely remove the VIIIE6$_2$ epitope from pamlin, as was shown by immunohistochemistry and immunoblotting. However, a perturbation of molecular properties did occur particularly at the 180 and 52 kDa subunits. Malformation of the 180 kDa subunit would not affect the morphogenetic activity of pamlin, since this subunit has no PMC-binding activity (Katow 1995). From the present immunoblots and Con A binding assay, the appearance of two VIIIE6$_2$-positive bands, one in the normal 52 kDa region and an additional one in the 47 kDa region, suggests that the mAb's epitope is found both in *N*-linked glycans (as seen in the additional 47 kDa fragment) and non *N*-linked glycans (as seen in preserved epitope in 52 kDa subunit) and that the mannose moieties are not the mAb's epitope.

A VIIIE6$_2$-positive 47-kDa band observed in tunicamycin-treated pamlin after immunoblotting was not visualized by silver or CBB stain. The mAb-binding fragment may possess molecular properties which make it unreactive with the silver and CBB stains as previously suggested by other authors (e.g. Hames 1990; Merril 1990).

These observations and the in vitro PMC-binding assay strongly indicate that fluctuation of the 52 kDa subunit associated with the splitting of the VIIIE6$_2$ epitope-carrier and the loss of *N*-linked glycans destroys the PMC-binding activity of pamlin, indicating a priori that *N*-linked glycans at the 52 kDa subunit constitute a molecular configuration crucial for the PMC-binding activity of this molecule.

The present study indicated that pamlin plays a major role in directing PMC migration and archenteron attachment during gastrulation. Although this protein is a major PMC-binding component in blastocoelic ECM, it is probably not the only molecule involved in early embryogenesis, since the sea urchin embryo has at least one more PMC-binding related protein, an FR-1 receptor, that locates quite similar histological sites to pamlin and recognizes the RGDS amino acid sequence (Yamamoto et al. 1995).

Acknowledgements This research was supported by a Rikkyo University Grant for the Promotion of Research. I thank the Misaki Marine Biological Station, University of Tokyo, for providing sea urchins throughout this research.

References

Amemiya S (1989) Development of the basal lamina and its role in migration and pattern formation of primary mesenchyme cells in sea urchin embryos. Dev Growth Differ 31:131–145

Bisgrove BW, Andrews ME, Raff RA (1991) Fibropellins, products of an EGF-containing gene, from a unique extracellular matrix structure that surround the sea urchin embryo. Dev Biol 146:89–99

Bronner-Fraser M (1986) Guidance of neural crest migration: Latex beads as probes of surface-substratum interactions. In: Browder LW (ed) Developmental biology: a comprehensive synthesis, vol 3. The cell surface in development and cancer. Plenum Press, New York, pp 301–338

Giudice G (1973) Developmental biology of the sea urchin embryo. Academic Press, New York

Hames BD (1990) One-dimensional polyacrylamide gel electrophoresis. In: Hames BD, Rickwood D (eds) Gel electrophoresis of proteins; a practical approach, 2nd edn. IRL Press, New York, pp 1–147

Hardin J (1988) The role of secondary mesenchyme cells during sea urchin gastrulation studied by laser ablation. Development 103:317–324

Hardin J, McClay DR (1990) Target recognition by the archenteron during sea urchin gastrulation. Dev Biol 142:86–102

Heifetz A, Lennertz WJ (1979) Biosynthesis of *N*-glycosydically linked glycoproteins during gastrulation of sea urchin embryos. J Biol Chem 254:6110–6127

Humphries MJ, Mould AP, Yamada KM (1991) Matrix in cell migration. In: McDonald JA, Meacham RP (eds) Receptors for extracellular matrix. Academic Press, San Diego, pp 195–253

Hynes RO (1990) Fibronectins. Springer, Berlin Heidelberg New York

Hynes RO, Lander AD (1992) Contact and adhesion specificities in the association, migration, and targeting of cells and axons. Cell 68:303–322

Karp GC, Solursh M (1985) Dynamic activity of the filopodia of sea urchin embryonic cells and their role in exploratory behavior of the primary mesenchyme in vitro. Dev Biol 112:276–283

Katow H (1986) Behavior of sea urchin primary mesenchyme cells in artificial extracellular matrices. Exp Cell Res 162:401–410

Katow H (1987) Inhibition of cell surface binding of fibronectin and fibronectin-promoted cell migration by synthetic peptides in sea urchin primary mesenchyme cells in vitro. Dev Growth Differ 29:579–589

Katow H (1990) A new technique for introducing anti-fibronectin antibodies and fibronectin-related synthetic peptides into the blastulae of the sea urchin, *Clypeaster japonicus*. Dev Growth Differ 32:33–39

Katow H (1995) Pamlin, a primary mesenchyme cell adhesion protein, in the basal lamina of the sea urchin embryo. Exp Cell Res 218:469–478

Katow H, Hayashi M (1985) Role of fibronectin in primary mesenchyme cell migration in the sea urchin. J Cell Biol 101: 1487–1491

Katow H, Nakajima Y (1992) Behavior and ultrastructure of primary mesenchyme cells at sessile site during termination of cell migration in early gastrulae. Dev Growth Differ 34:107–114

Katow H, Solursh M (1979) Ultrastructure of blastocoel material in blastulae and gastrulae of the sea urchin, *Lytechinus pictus*. J Exp Zool 210:561–567

Katow H, Solursh M (1982) In situ distribution of concanavalin A-binding sites in mesenchyme blastulae and early gastrulae of the sea urchin, *Lytechinus pictus*. Exp Cell Res 139:171–180

Katow H, Yazawa S, Sofuku S (1990) A fibronectin-related synthetic peptide, Pro-Ala-Ser-Ser, inhibits fibronectin binding to the cell surface, fibronectin-promoted cell migration in vitro, and cell migration in vivo. Exp Cell Res 190:17–24

Katow H, Yazawa S, Sofuku S (1991) Inhibition of cell surface binding of fibronectin and fibronectin-promoted cell migration in vitro by a fibronectin-related synthetic peptide, Pro-Ala-Ser-Ser, in the sea urchin, *Pseudocentrotus depressus*. St Paul's Rev Sci 31:1–10

Laemmli UK (1970) Cleavage of structural proteins during the assembly of the bacteriophage T4. Nature 227:680–685

Lane MC, Solursh M (1988) Dependence of sea urchin primary mesenchyme cell migration on xyloside- and sulfate-sensitive cell surface-associated compound. Dev Biol 127:78–87

Lane MC, Solursh M (1991) Primary mesenchyme cell migration requires a chondroitin sulfate/dermatan sulfate proteoglycan. Dev Biol 143:389–397

Lee HC, Epel D (1983) Changes in intercellular acidic compartments in sea urchin eggs after activation. Dev Biol 98:446–454

McCarthy RA, Beck K, Burger MM (1987) Laminin is structurally conserved in the sea urchin basal lamina. EMBO J 6:1587–1593

McClay DR (1993) Assembly of the extracellular matrix following fertilization of the sea urchin embryo. J Reprod Dev Suppl 39:85–86

Merril CR (1990) Gel stain technique. In: Deutcher MP (ed) Methods in enzymology, vol 182. Guide to protein purification. Academic Press, San Diego, pp 477–488

Nakajima Y, Katow H (1991) Initial characterization of primary mesenchyme cell homing site in sea urchin blastulae. In: Yanagisawa K, Yasumasu I, Oguro C, Suzuki N, Motokawa T (eds) Biology of echinodermata. Balkema, Rotterdam, pp 461–466

Newgreen DF (1990) Control of the directional migration of mesenchyme cells and neurites. Semin Dev Biol 1:301–311

Okazaki K, Fukushi T, Dan K (1962) Cyto-embryological studies of sea urchins. IV. Correlation between the shape of the ectodermal cells and the arrangement of the primary mesenchyme cells in sea urchin larvae. Acta Embryol Morphol Exp 5:17–31

Shimizu-Nishikawa K, Katow H, Matsuda R (1990) Micromere differentiation in the sea urchin embryo: immunochemical characterization of primary mesenchyme cell-specific antigen and its biological roles. Dev Growth Differ 32:629–636

Soltysik-Espanola M, Klinzing DC, Pfarr K, Burk RD, Ernst SG (1994) Endo 16, a large multidomain protein found on the surface and ECM of endodermal cells during sea urchin gastrulation, binds calcium. Dev Biol 165:73–85

Solursh M (1986) Migration of sea urchin primary mesenchyme cells. In: Browder LW (ed) Developmental biology. A comprehensive synthesis. Plenum Press, New York, pp 391–432

Solursh M, Lane MC (1988) Extracellular matrix triggers a directed cell migratory response in sea urchin primary mesenchyme cells. Dev Biol 130:397–401

Struck DK, Lennarz WJ (1981) The function of saccharide-lipids in synthesis of glycoproteins. In: Lennarz WJ (ed) The biochemistry of glycoproteins and proteoglycans. Plenum Press, New York, pp 35–83

Towbin H, Staehelin T, Gordon J (1979) Electrophoretic transfer of proteins from acrylamide gels to nitrocellulose sheets: procedure and applications. Proc Natl Acad Sci USA 76:4350–4354

Welply JK, Lau JT, Lennarz WJ (1985) Developmental regulation of glycosyltransferases involved in synthesis of *N*-linked glycoproteins in sea urchin embryos. Dev Biol 107:252–258

Wessel GM, McClay DR (1987) Gastrulation in the sea urchin embryo requires the deposition of crosslinked collagen within the extracellular matrix. Dev Biol 121:149–165

Yamamoto Y, Katow H, Sofuku S (1995) Synthesis of RGDS-PASS-containing cysteine peptides and isolation of RGD-recognizing receptor in sand dollar embryo by the peptide-affinity chromatography. Chem Lett 1995:483–484